Proceedings of the ASME 2020 39th International Conference on Ocean, Offshore and Arctic Engineering
OMAE2020
August 3-7, 2020, Virtual, Online

OMAE2020-18173

LEADING EDGE EROSION OF WIND TURBINE BLADES: EFFECTS OF ENVIRONMENTAL PARAMETERS ON IMPACT VELOCITIES AND EROSION DAMAGE RATE

Amrit Shankar Verma*
Delft University of Technology (TU Delft)
Faculty of Aerospace Engineering
Delft, Netherlands
Email: a.s.verma@tudelft.nl

Zhiyu Jiang
University of Adger
Department of Engineering Sciences
Grimstad, Norway
Email: zhiyu.jiang@uia.no

Zhengru Ren
NTNU
Department of Marine Technology
Trondheim, Norway
Email: zhengru.ren@ntnu.no

Julie J.E. Teuwen
Delft University of Technology (TU Delft)
Faculty of Aerospace Engineering
Delft, Netherlands
Email: J.J.E.Teuwen@tudelft.nl

ABSTRACT

Leading edge erosion (LEE) of a wind turbine blade (WTB) is a complex phenomenon that contributes to high operation and maintenance costs. The impact between rain droplets and rotating blades exerts cyclic fatigue stresses on the leading edge - causing progressive material loss and reduced aerodynamic performance. One of the most important parameters for erosion modelling and damage prediction is the relative impact velocity between rain droplets and rotating blade and depends upon the environmental conditions. The environmental condition, in general, could vary for onshore and offshore wind turbines (OWTs) - for instance, the presence of wave-induced loads along with less turbulent wind and varying rainfall conditions in the offshore environment. The present paper tries to provide guidelines whether all these parameters need to be included for LEE modelling. Aero-hydro-servo-elastic simulations are carried out for a rotating blade based on the NREL 5 MW turbine by considering realistic environmental conditions for a land-based wind turbine and monopile-supported OWT. Further, the impact velocities and erosion damage rate, evaluated using a surface fatigue model, are analysed and compared for different environmental conditions. It is found that rainfall intensity and turbulence intensity influences the impact velocity minorly, however, has a substantial effect on the overall erosion damage rate. For instance, for the investigated load cases, an 8% increase in the impact velocity is observed when the turbulence intensity increases from 6% to 26%, which indicates an increase of erosion damage rate by more than 40%. Furthermore, no substantial influence is found due to the effects of wave-induced loads on the wind turbine.

INTRODUCTION

The consistent demand in the renewable sources of energy has led to rapid increase in the exploitation of power from sustainable sources such as wind, hydro, wave and solar [1]. Among different resources, wind energy is one of the most reliable and readily available, and can be harnessed using wind turbines [2,3] (Figure 1(a)). The principle for energy extraction through wind turbines involves converting the kinetic energy of the wind into mechanical energy through the rotation of the blades, and finally harnessing this into usable electrical energy by means of genera-

*Address all correspondence to this author.

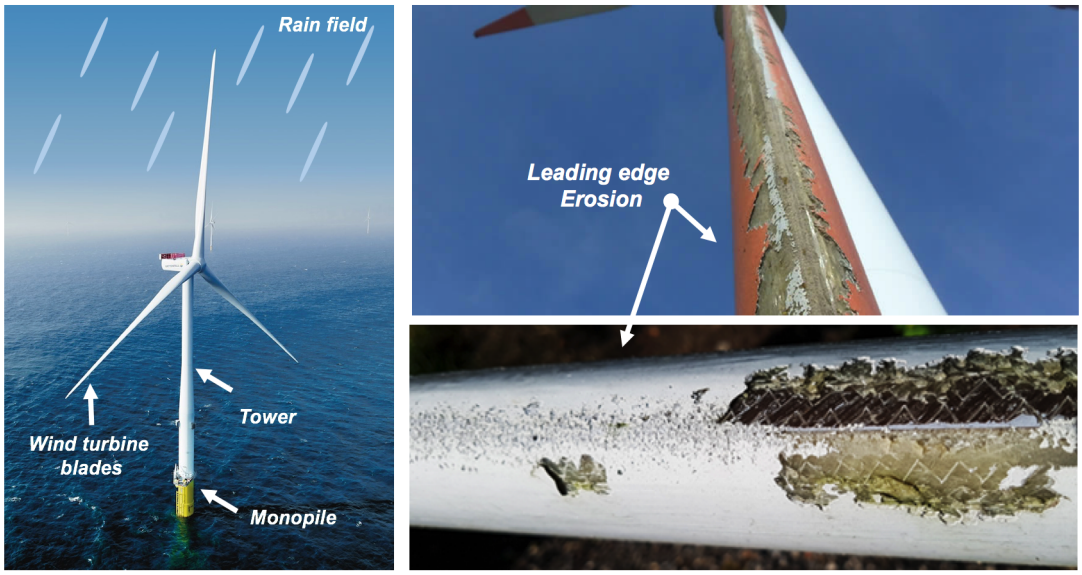

FIGURE 1: Examples of leading edge erosion of wind turbine blades [4–6]

tors present in the nacelle. Given that the power extracted from a turbine increases with the rotor swept area along with cube of the wind speed, large size turbines are currently in high demand both in onshore and offshore sectors [7, 8]. For instance, the average rated capacity for installed offshore wind turbines (OWTs) in Europe has increased from 4.2 MW in 2014 to 6.8 MW at the end of 2018, with 10 MW turbines currently in operation [9].

This upscaling in the size of wind turbines is profitable, however, it poses several engineering challenges especially related to their design aspects. For instance, a typical 10 MW turbine can have blade length in the range of 70-100 meters, and they must be designed stiff enough to negate collision with tower during their mechanical rotation under the action of wind-induced flapwise loads. In addition, these large size blades are susceptible to material degradation due to exposure to harsh environmental conditions in the forms of rain (Figure 1(a)), UV or hail impact [10]. The issue becomes critical as the latest generation blades rotate with tip speeds in the range of 65-110 m/s. The impacts between rain droplet and rotating blades at such high velocities, during the service life, exert cyclic fatigue stresses on the blade eventually causing their leading edge erosion (LEE) [11].

Leading edge erosion (LEE) of a wind turbine blade (WTB) is a critical issue that causes development of pitting and surface cracks at the leading edge (Figure 1(b)) and in severe cases the damage could even penetrate into the composite substrate (Figure 1(b)) [12]. LEE causes the local roughening of surfaces, which in turn provokes premature transition of laminar flow into turbulent flow along the leading edge - thereby reducing the aerodynamic efficiency and annual energy production (*AEP*) of a turbine [13]. In general, regular inspection, maintenance and repair of WTBs due to LEE is inevitable to keep up with the target *AEP* of a turbine through the design life - thereby making the energy produced from the wind turbine expensive. It has been reported by [13, 14] that repair and maintenance due to LEE costs European OWT sector more than £56 million annually- therefore LEE of WTBs requires immediate attention.

To tackle the issue of LEE due to high velocity rain droplet impact, several research efforts are being made. These include developing, testing and comparing leading edge coating systems in accelerated rain erosion tests, and quantifying their rain erosion resistance in excess of 100-200 m/s droplet impact [15–17]. Another aspect for controlling rain erosion of WTB is to develop control algorithm [18], which automatically reduces the tip speed of the blade (and thus the impact velocity) in the event of harsh precipitation, thereby inhibiting cumulative fatigue damage accumulation due to repeateted rain droplet impact. Computational models [12, 19] are also being developed where emphasis is to estimate the fatigue life based on cyclic stresses induced on the leading edge over its service life.

Amirzadeh et. al [21] developed a computational framework to estimate fatigue life of blade, where erosion damage rates for the leading edge under varying impact velocities and different rainfall conditions were evaluated. Similar studies can also be found in [16, 22–24] where fluid structure interaction models are developed using sophisticated numerical codes. However, one of the simplifications in all the previous studies is that a maximum impact velocity between 100-140 m/s is simply assumed for analysis purposes and the effects of droplet impact angles

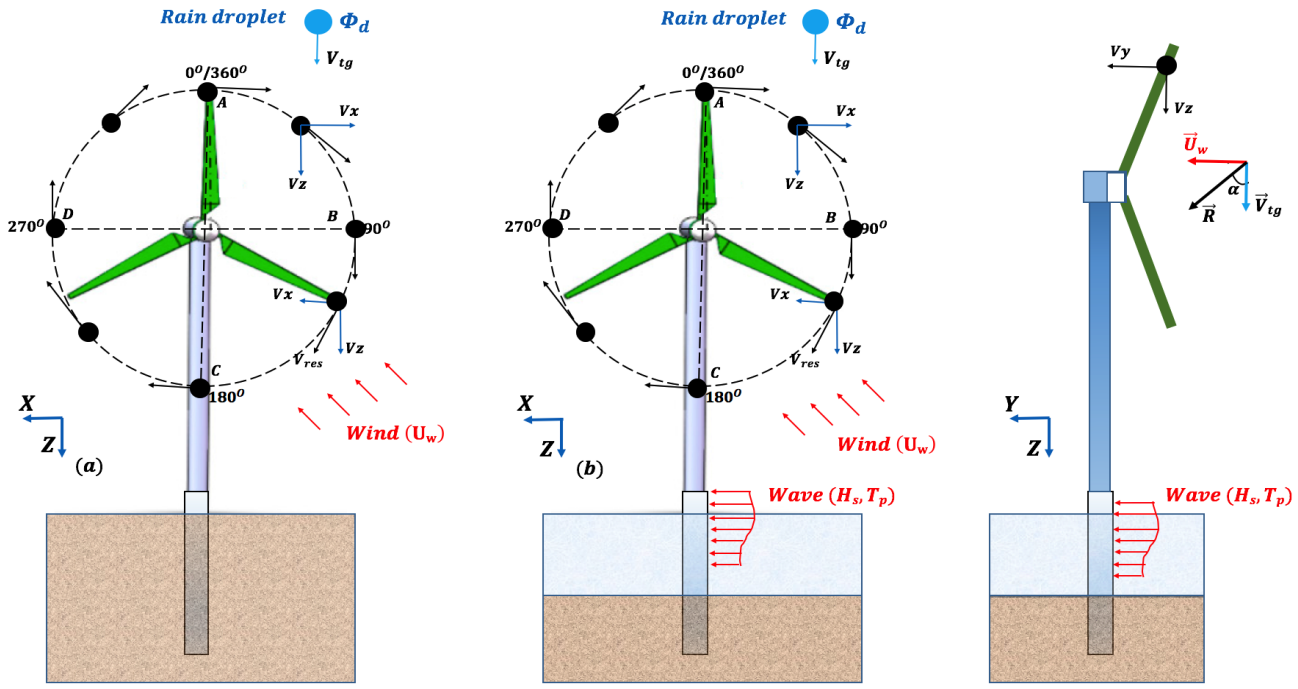

FIGURE 2: Different input variables related to onshore and OWTs (Modified figure from [20]) and definition of impact angle α

and blade rotation are ignored. In principle, for fatigue design of the coating material, it is essential to quantify the impact velocity and their cyclic variation during the blade rotation as well as their dependence on rainfall intensity and droplet impact angle. It has been proved in the literature [11, 17] that damage erosion rate ($\dot{D}_i$) of leading edge is proportional to impact velocity ($\vec{V}_{imp}$) by a power of almost seven times ($|\vec{V}_{imp}|^{6.7}$). Therefore, this makes $\vec{V}_{imp}$ as one of the most important parameters for erosion modelling and damage prediction of leading edge.

In principle, $\vec{V}_{imp}$ depends on the environmental conditions a wind turbine (WT) is exposed to and this could vary for onshore and OWT. For instance, the presence of wave loads (Figure 2) along with less turbulent wind and varying rainfall conditions in the offshore environment. This poses the question if there are any differences in impact velocities and erosion damage rates of a WTB due to - (a) different rainfall intensities (b) turbulence intensities, and (c) wave-induced loads and how does each parameter influence LEE during blade rotation. The present paper tries to answer this question and provides guidelines whether all these parameters need to be included for LEE modelling. Aero-hydro-servo-elastic simulations are carried out for a rotating blade based on the NREL 5 MW turbine for a land-based WT and a monopile-supported OWTs. The relative impact velocity between the rain droplet and rotating blade along with erosion damage rate based on a surface fatigue model are compared for different rainfall intensities and blade azimuth angle.

PROBLEM DEFINITION AND ANALYSIS PROCEDURE

There are two main parameters that are of interest for the LEE of WTBs and are - (a) relative impact velocity between rain droplet and rotating blades ($\vec{V}_{imp}$), and (b) droplet impact responses and associated LEE damage rate ($\dot{D}_i$). These parameters are defined below:

I. Relative impact velocity between rain droplet and rotating blade ($\vec{V}_{imp}$)

$\vec{V}_{imp}$ depends upon following input variables: (**1**) environmental conditions consisting of significant wave height (H_s), spectral wave peak period (T_p), mean wind speed (U_w) and turbulence intensity (TI), (**2**) the rainfall intensity (I), (**3**) droplet diameter (ϕ_d), (**4**) droplet impact angle (α), (**5**) terminal velocity of rain droplet ($\vec{V}_{tg}$), and finally (**6**) design power curve of a WT which governs the rotational speed of blade during operation. Further, for a given wind turbine and as a result of these variables, $\vec{V}_{imp}$ would vary with blade azimuth angle ($\theta \in [0^o, 360^o]$) and at different positions (r) along the blade length (l).

The relative impact velocity between rain droplet and rotating blade ($\vec{V}_{imp}$) is given by the following equation (Figure 2):

$$|\vec{V}_{imp}| = \sqrt{(V_x)^2 + (V_y - |\vec{R}|\, sin\alpha)^2 + (V_z - |\vec{R}|\, cos\alpha)^2} \quad (1)$$

where V_x, V_y, and V_z are rotational velocity components of the blade in global-x, y and z direction. For simplicity, V_x is neglected

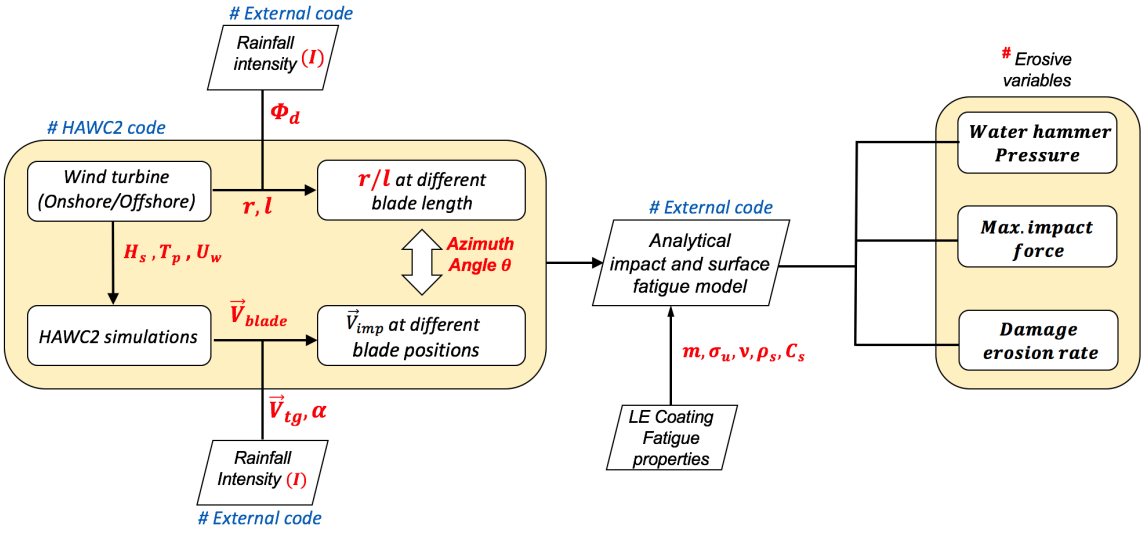

FIGURE 3: Analysis procedure considered in the study

in this study for estimating the relative impact velocity, as this component is not affected by varying the rainfall characteristics. α is defined as the droplet impact angle, and is defined as [25] (see Figure 2):

$$\alpha = arctan \frac{|\vec{U}_w|}{|\vec{V}_{tg}|} \tag{2}$$

where $\vec{U}_w$ is the horizontal mean wind speed, and $\vec{V}_{tg}$ is defined as the terminal velocity of a droplet in the normal direction to the ground. $|\vec{R}|$ is defined as the resultant vector between $|\vec{U}_w|$ and $|\vec{V}_{tg}|$. $\vec{V}_{tg}$ is given by:

$$\vec{V}_{tg} = 9.65 - 10.3e^{-0.6\phi_d} \quad (0.5mm < \phi_d < 5mm) \tag{3}$$

where ϕ_d is defined as the representative droplet diamater for a given rainfall intensity (I). It is to be noted that for simplicity, the normal velocity of the droplet is assumed to be the mean wind speed rather than the local wind speed, whereas the terminal velocity of the droplet ($\vec{V}_{tg}$) is empirical defined by eq. 3. It is possible to obtain the local wind velocity at the blade tip and use it in the relative impact velocity. However, there will be uncertainties associated with the turbulent wind field. Furthermore, the rain droplet diameter (ϕ_d) is related to rainfall intensity (I) through a distribution given by Best distribution [26]:

$$F(\phi_d) = 1 - e^{-\left(\frac{\phi_d}{1.3 * I^{0.232}}\right)^{2.25}} \tag{4}$$

where $F(\phi_d)$ is the cumulative distribution function (CDF) of droplet size. Note that recently Herring et al. [27] presented a CDF for ϕ_d for offshore conditions, as well as compared the estimates from Best [26], and notable differences were found. The Best's distribution has been used extensively in all the literature reports in the past, and data for analysis in [27] for offshore conditions are based on only one year of recorded data, and requires further improvement. Therefore, in this study, the Best's distribution [26] is used for selecting suitable droplet size for both onshore and offshore conditions. It is to be also noted that the current study assumes droplets as spherical for all the cases. However, there could be changes in the shape of the droplet especially for larger size droplets and could affect the droplet terminal velocity. All the variables discussed through these equations are also marked in a flow chart shown in Figure 3, where analysis framework of the study is described. First, aero-hydro-servo-elastic simulations are carried out in HAWC2 [28] for a rotating blade based on NREL 5 MW turbine [29] by considering realistic environmental conditions for land-based WT and monopile-supported OWT. From the analysis, rotational speed of the blade (V_z, V_y) are evaluated at different θ along the blade span length (r/l). Further, these results are combined with an inhouse external code describing rainfall parameters - ϕ_d, I, α and $\vec{V}_{tg}$, and $|\vec{V}_{imp}|$ is estimated using eq. (1). The details of environmental load cases are described in the next section. Once, $|\vec{V}_{imp}|$ is evaluated, structural responses of the leading edge due to rain droplet impact are evaluated for different environmental parameters.

II. Droplet impact responses and associated LEE damage rate ($\dot{D}_i$)

Following are the LE structural response parameters that are used to quantify LEE damage: (1) peak impact forces (F_{imp}), (b) water hammer pressure (p_{wh}), and (c) damage erosion rate (D_i)(Figure 3). The F_{imp} on the blade's leading edge is given by

an analytical model developed by [30, 31]. The analytical model is verified in our previous work [22] and F_{imp} is given as:

$$F_{imp} = 0.84\,\rho_w\,|\vec{V}_{imp}|^2\,\phi_d^2 \tag{5}$$

where, ρ_w is the density of water taken as $1000kg/m^3$. Further, the erosion damage rate is defined by an analytical surface fatigue damage model developed and validated by [11, 17]. The model applies Miner's rule to estimate $\dot{D}_i$ and is given by:

$$\dot{D}_i = \frac{\dot{N}}{N_{ic}} = \frac{q|\vec{V}_{imp}|\beta_d}{\frac{8.9}{\phi_d^2}\left(\frac{S}{P}\right)^{5.7}} \tag{6}$$

where, $\dot{D}_i \geq 1$ implies fatigue damage, q is the number of droplets per unit volume of rainfall which is given by:

$$q = 530.5\frac{I}{V_{tg}\phi_d^3} \tag{7}$$

β_d is the impingement efficiency given by the relation:

$$\beta_d = 1 - e^{-15\phi_d} \tag{8}$$

P_{wh} is the water hammer pressure defined by:

$$P_{wh} = \frac{\rho_w c_w |\vec{V}_{imp}|}{1 + \frac{\rho_w c_w}{\rho_s c_s}} \tag{9}$$

where ρ_s and c_s are density and speed of sound in the coating material respectively. S is the erosive strength of coating material defined by:

$$S = \frac{4\sigma_u(m-1)}{1-2\nu} \tag{10}$$

σ_u, m and ν are the ultimate strength, Wohler slope and Poisson's ratio of the coating material. In this study, a Polyethylene Terephthalate (PET) based thermoplastic coating material [15] is used to determine the erosion damage rate. The material properties are derived from [15] and tabulated in Table 1.

MATERIAL AND MODELLING METHOD

A generic 5MW based wind turbine originally designed by NREL is modelled in aeroelastic HAWC2 code [28] for estimating global motion responses of the rotating blade for both onshore and OWT. The code is based on multibody dynamics where

Table 1: *Material properties for coating material [15]*

Parameter	Values	Units
ρ_s	1320	kg/m^3
c_s	2480	m/s
σ_u	57.6	MPa
m	14.9	-
ν	0.395	-

structural systems can be discretised with timoshenko beam elements and components of the turbine can be connected together through constraints or joints [32]. The code is able to simulate time domain responses of wind turbines under the action of aerodynamic as well as hydrodynamic loads. The design parameters for the NREL 5 MW wind turbine are are provided in Table 2.

Figure 4 presents the numerical model for OWT considered in

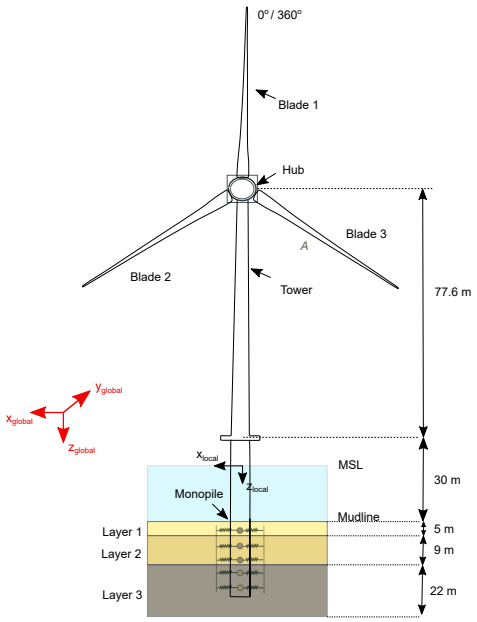

FIGURE 4: Numerical model considered in HAWC2 for OWT

the study, where the NREL 5 MW turbine [29] is adapted based on phase II model of Offshore Code Comparison (OC3) [33]. Realistic soil properties are defined for the monopile, having a diameter of 9 m. An eigenfrequency analysis is performed for the OWT turbine and the natural period in first fore-aft and side-side bending mode is found to be around 4.2 s (T_{FA}, $T_{SS} = 4.2s$). It is to be noted that in the original OC3 model, the damping ratio of the first fore-aft and side-side bending mode of the turbine is close to 0.2%, which is tuned to value of 1% critical

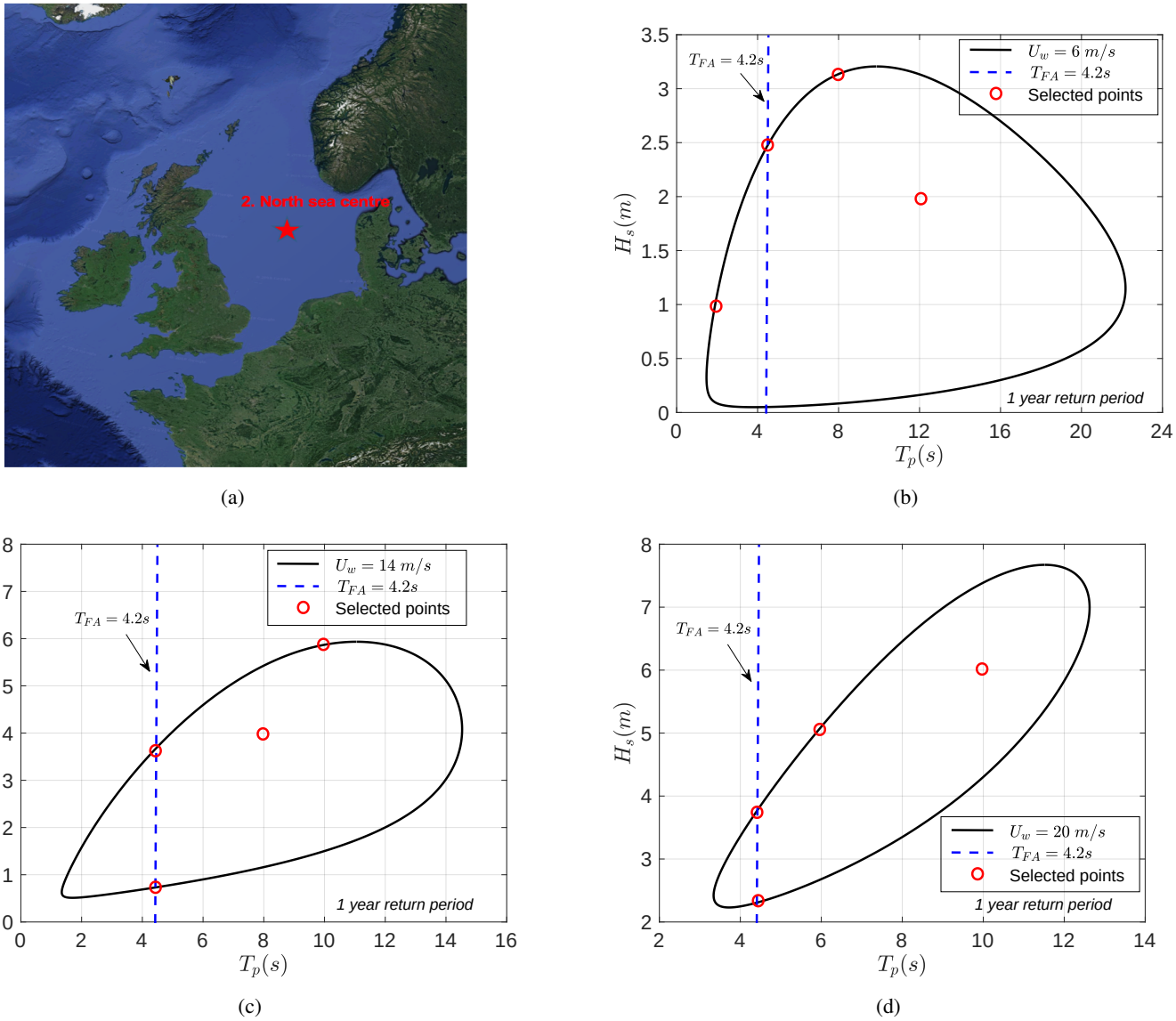

FIGURE 5: (a) North sea centre offshore site; 2D contour surface for H_s, T_p for (a) U_w=6m/s (b) U_w=14m/s (c) U_w=20m/s and selected load cases

in this study as per recommendations and experimental observations from [34]. The structural components including blades, monopile and tower are modelled using timoshenko beam elements, and soil is defined through distributed springs. The hydrodynamic loads on the monopile are calculated by Morison's equation [35] and the JONSWAP spectrum is used to generate the irregular wave. Further, in HAWC2 simulations [36], aerodynamic loads on the blade are evaluated using Blade Element Momentum (BEM) theory with engineering corrections. The BEM implemented in HAWC2 includes several engineering models such as dynamic inflow (dynamic induction), skew inflow, dynamic stall and the near-wake model. The efficiency of these models in HAWC2 are validated against CFD and advanced vortex model for blade load and axial induction; see [37, 38]. However, note that BEM cannot account for advanced flow effects like wake rotation and hence may affect the local flow phenomenon, but the corrected BEM is still useful for engineering aeroelastic analysis. Furthermore, inflow wind turbulence is generated using Mann's turbulence box in HAWC2 code, and effects of wind shear are included. The details of the parameters used for generating the turbulence can be found in another work [2]. Also, note that the model for onshore wind turbine is similar to OWT except that: (1) the tower of the land-based turbine is rigidly connected at the bottom, (2) and there are no hydrodynamic loads acting on the turbine.

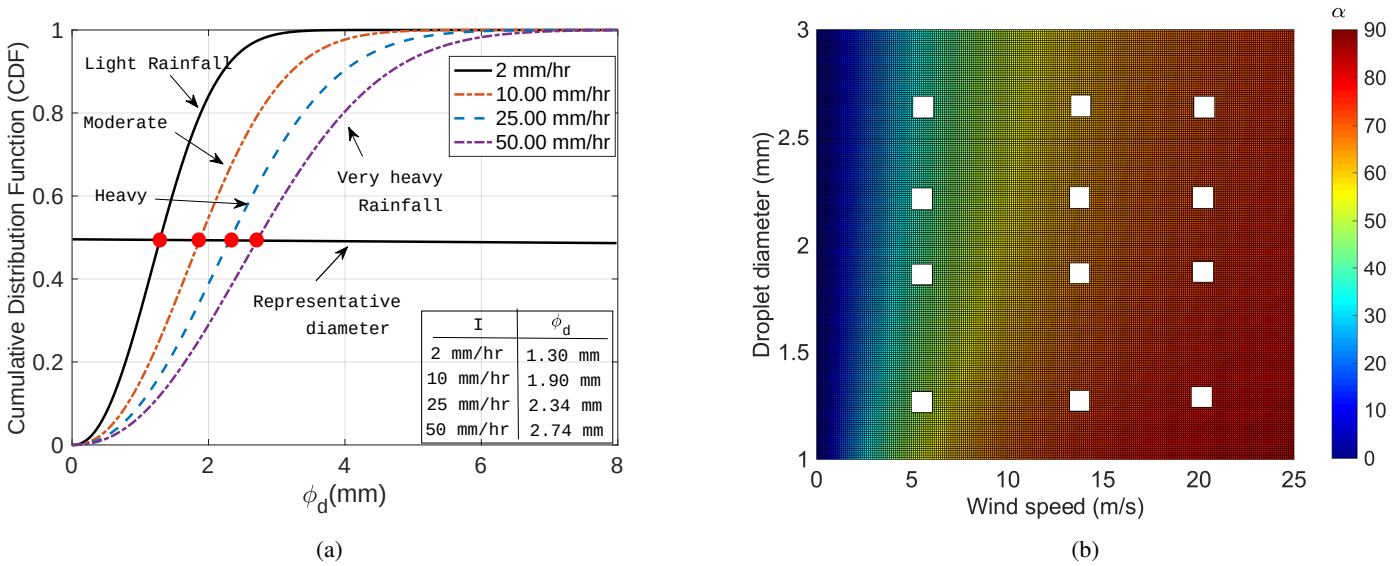

(a) (b)

FIGURE 6: (a) Choice of ϕ_d for different I (b) Variation of α (*degrees*) with varying ϕ_d and U_w

Table 2: *Description of NREL 5-MW reference turbine [29]*

Rating	5MW turbine
Rotor orientation, configuration	Upwind, 3 Blades
Control Variable speed	Collective pitch
Drivetrain High speed	Multiple-stage gearbox
Rotor, Hub diameter	126 m, 3 m
Hub height	90 m
Cut-in, Rated, Cut-out wind speed	3 m/s, 11.4 m/s, 25 m/s
Cut-in, Rated rotor speed	6.9 rpm, 12.1 rpm
Rated tip speed	80 m/s
Rotor mass	110,000 kg
Nacelle mass	240,000 kg
Tower mass	347,460 kg

Table 3: *Load cases considered for the analysis*

EC	$U_w\ (m/s)$	TI	$H_s\ (m)$	$T_p\ (s)$
EC1	6	0, 0.06, 0.12, 0.26	1.00	2.00
EC2	6	0, 0.06, 0.12, 0.26	2.30	4.20
EC3	6	0, 0.06, 0.12, 0.26	3.14	8.00
EC4	6	0, 0.06, 0.12, 0.26	2.00	12.00
EC5	14	0, 0.06, 0.12, 0.26	0.70	4.20
EC6	14	0, 0.06, 0.12, 0.26	3.50	4.20
EC7	14	0, 0.06, 0.12, 0.26	4.00	8.00
EC8	14	0, 0.06, 0.12, 0.26	6.00	10.00
EC9	20	0, 0.06, 0.12, 0.26	2.27	4.20
EC10	20	0, 0.06, 0.12, 0.26	4.90	4.20
EC11	20	0, 0.06, 0.12, 0.26	5.00	6.00
EC12	20	0, 0.06, 0.12, 0.26	6.00	10.00

Environmental load cases

Wave and wind conditions: For analysing LEE subjected to rain droplet impact for onshore and offshore wind turbine, three different mean wind speeds i.e, $U_w = 6,\ 14,\ 20\ m/s$ are considered in this study. These cases range between the cut-in and rated wind speed of a turbine ($U_w = 6m/s$), rated and cut-off speed ($U_w = 14m/s$), and the last one being closer to the cut-off speed ($U_w = 20m/s$). Further, for each case of U_w, four different TI are considered ($TI = 0,\ 0.06,\ 0.12,\ 0.26$). These values represent steady wind, and wind with low, medium and high turbulences respectively. For instance, $TI = 0.06$ represents turbulence level at which OWT operates, while $TI = 0.26$ corresponds to inflow wind conditions during gust and storm. For considering the effects of wave loads, the North-sea centre is considered as a representative offshore site (Figure 5(a)), and the 2D contour surface [3] for different combinations of H_s and T_p for the chosen U_w are shown in Figures 5(b)-(d). The red dots in the Figures 5(b)-(d) correspond to the selected load cases for OWT. Note that the points where the vertical line intersects the contour surface corresponds to the case close to the highest resonance frequency of the turbine ($T_{FA} = 4.2s$). Overall, there were twelve load cases (EC1 to EC12) considered and given in Table 3. Also, for each load case, there were 20 random seeds analysed for considering statistical uncertainty. Each analysis is run for 4000 s,

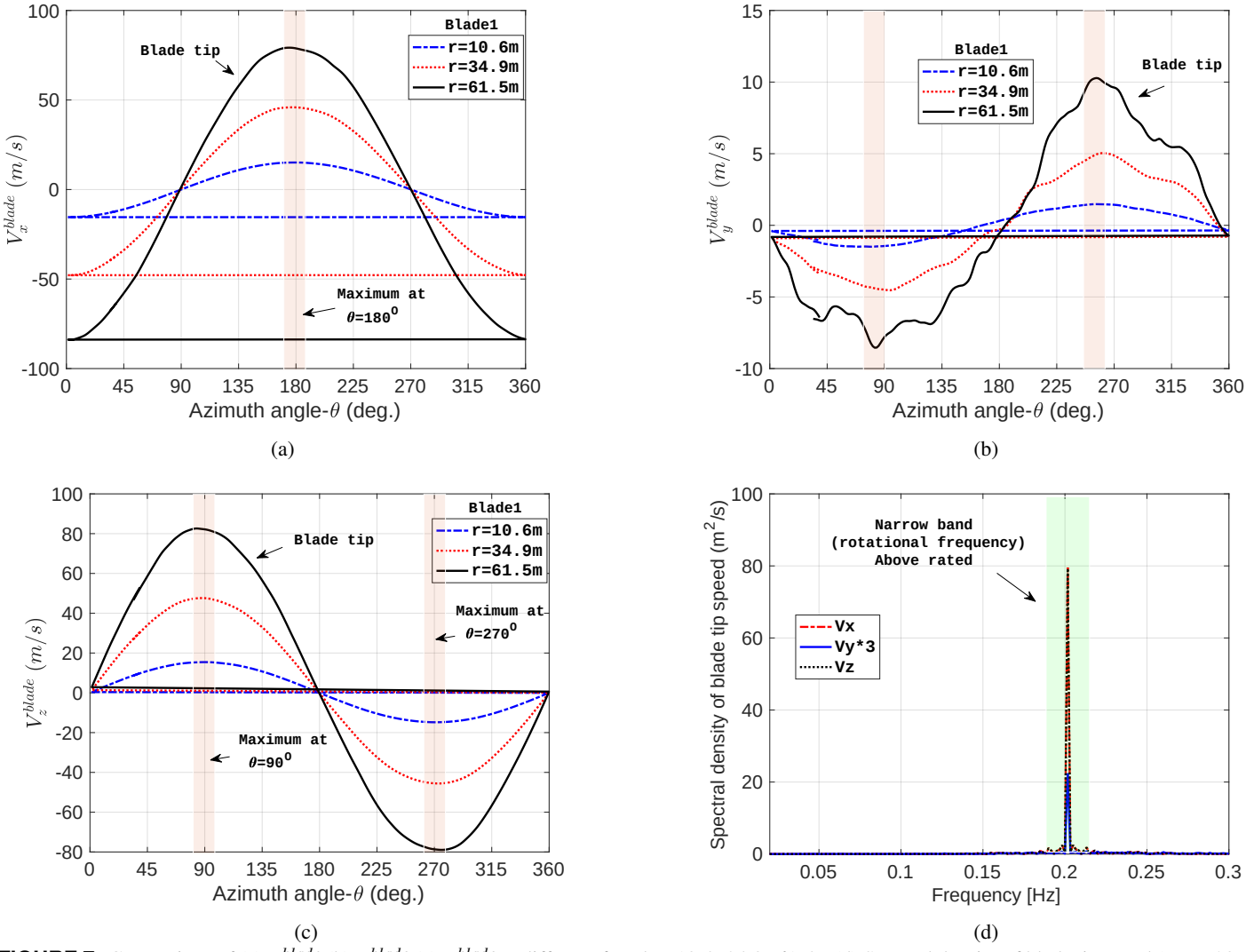

FIGURE 7: Comparison of (a) V_x^{blade} (b) V_y^{blade} (c) V_z^{blade} at different θ and r= 10.4, 34.9, 61.5m (d) Spectral density of blade tip speed ($U_w = 20m/s$)

where the first 400 s are filtered out to avoid start-up effects.

Rainfall conditions: Four different rainfall intensities (I) are considered for both onshore and OWT - (1) Light rainfall (2 mm/hr), (b) moderate rainfall (10 mm/hr), (c) heavy rainfall (25 mm/hr), and (d) very heavy rainfall (50 mm/hr). Based on these I, rain droplet size (ϕ_d) is determined from the distribution given by eq. (4), and is shown in Figure 6(a). The points where the black horizontal line intersects the CDF curve corresponds to representative ϕ_d considered in the study i.e, ϕ_d = 1.30, 1.90, 2.34, 2.74mm for different I. Further, $\vec{V}_{tg}$ are obtained for different ϕ_d from eq. (3), based on which droplet impact angles (α) are evaluated for different U_w. Figure 6(b) presents α for various cases of ϕ_d and U_w, where white dots in the figure represent the values considered in the present study.

RESULTS AND DISCUSSION

In this section, the results for the velocities of rotating blade are presented first and are discussed at different azimuth angle and blade positions. Further, the effects of: (a) rainfall intensity (b) wave-induced loads, and (c) turbulence intensity, on impact velocities and erosion damage rate are discussed. Note that for all the cases '*Blade* 1' of the turbine is used for discussion.

I. Blade speed at different azimuth angles (θ) and blade positions (r)

Figures 7(a)-(c) present the blade velocity in the global x, y and z-direction respectively for the case of $U_w = 20m/s$, TI = 0.06, and corresponding to an onshore wind turbine. The results are presented at different blade azimuth angles (θ), and three

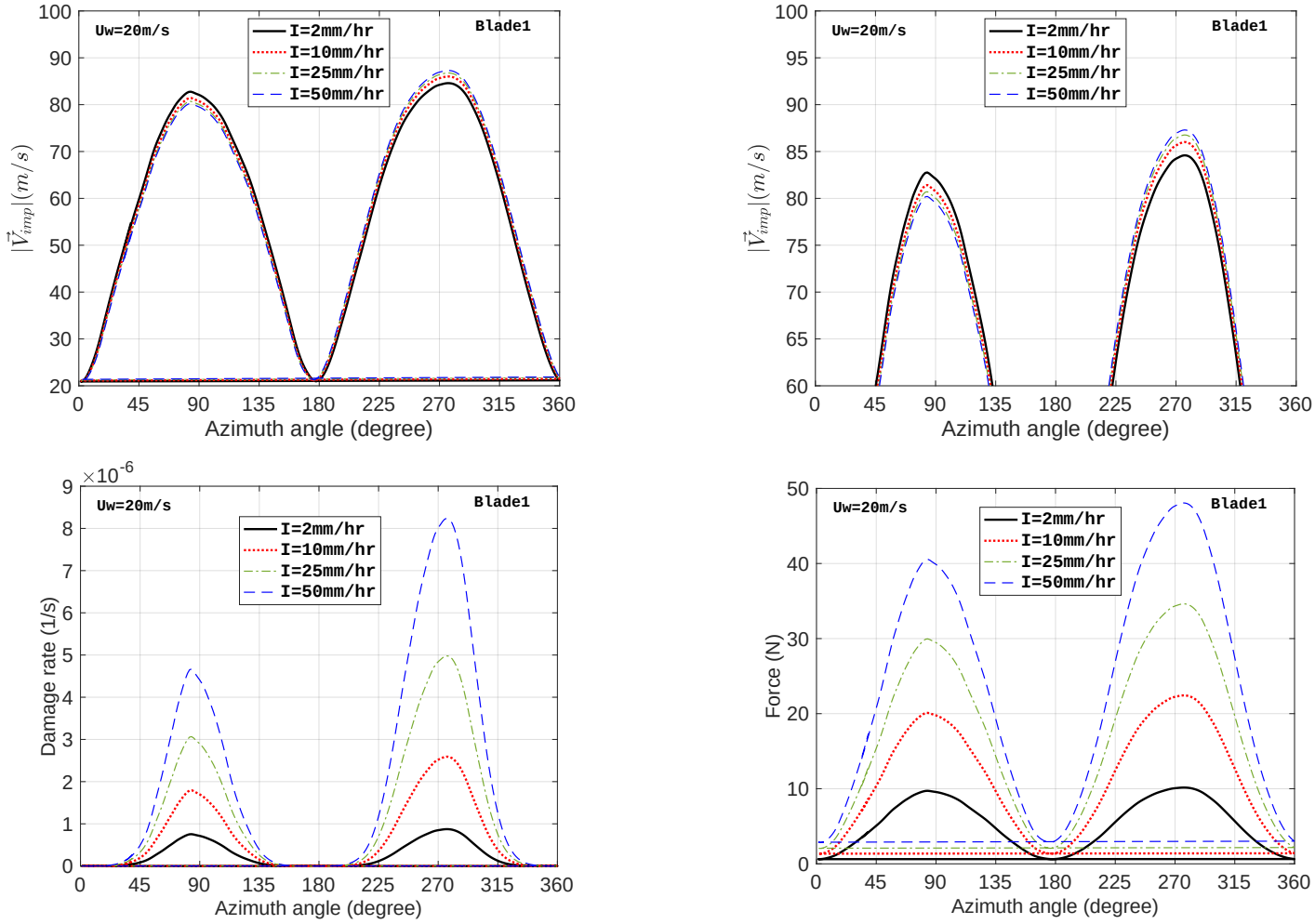

FIGURE 8: Comparison of (a) $|\vec{V}_{imp}|$ for $I = 2mm/hr,\ 10mm/hr,\ 25mm/hr,\ 50mm/hr$ (b) magnified view; comparison of (c) $\dot{D}_i$ (d) F_{imp}

different positions along the blade length. It can be seen that the velocity of the rotating blade is highest in the rotor-plane (xz), with blade velocity largest in x and z direction. On the other hand, the velocity of the blade in the global y-direction (V_y^{blade}) is relatively smaller and its peak value is close to 11 m/s compared to V_x and V_z where peak velocity can be in the range of 80 m/s.

Also, as expected, blade tip shows the largest velocity for all the cases, and thus will be used for discussion of results in subsequents sections. Furthermore, the velocity of the blade in x-direction has the positive peak value at $\theta = 180^o$ and negative peak value at $\theta = 0^o$. On the other hand, V_z^{blade} has the highest positive impact velocity at $\theta = 90^o$, and corresponding negative velocity at $\theta = 270^o$. This negative velocity at $\theta = 270^o$ is expected to give the largest relative impact velocity between rain and the rotating blade ($\vec{V}_{imp}$), due to the direction of rainfall in the opposite direction. Note that it is V_y^{blade} and V_z^{blade} that influences the $\vec{V}_{imp}$ (see eq.(1)) for varying rainfall characteristics, hence only these will be discussed further. It is also seen from the figure that V_z^{blade} shows a perfect smooth sinusoidal curve. However, V_y^{blade} is affected by TI, and thus a perfect sinusoidal smooth function is not obtained, the effect of which is critical at the blade tip. Nevertheless, the spectral density curve of the blade tip speed shown in Fig. 7(d) clearly shows its narrow band behaviour and represents the dominating frequency defined by the power curve of WT.

II. Effects of rainfall intensity (I)

Figure 8(a) presents the comparison between relative impact velocity between rotating blade tip ($r = 61.5m$) and rain droplet corresponding to different rainfall intensities ($I = 2mm/hr,\ 10mm/hr,\ 25mm/hr,\ 50mm/hr$). The results are presented at different θ and for a case of onshore wind turbine op-

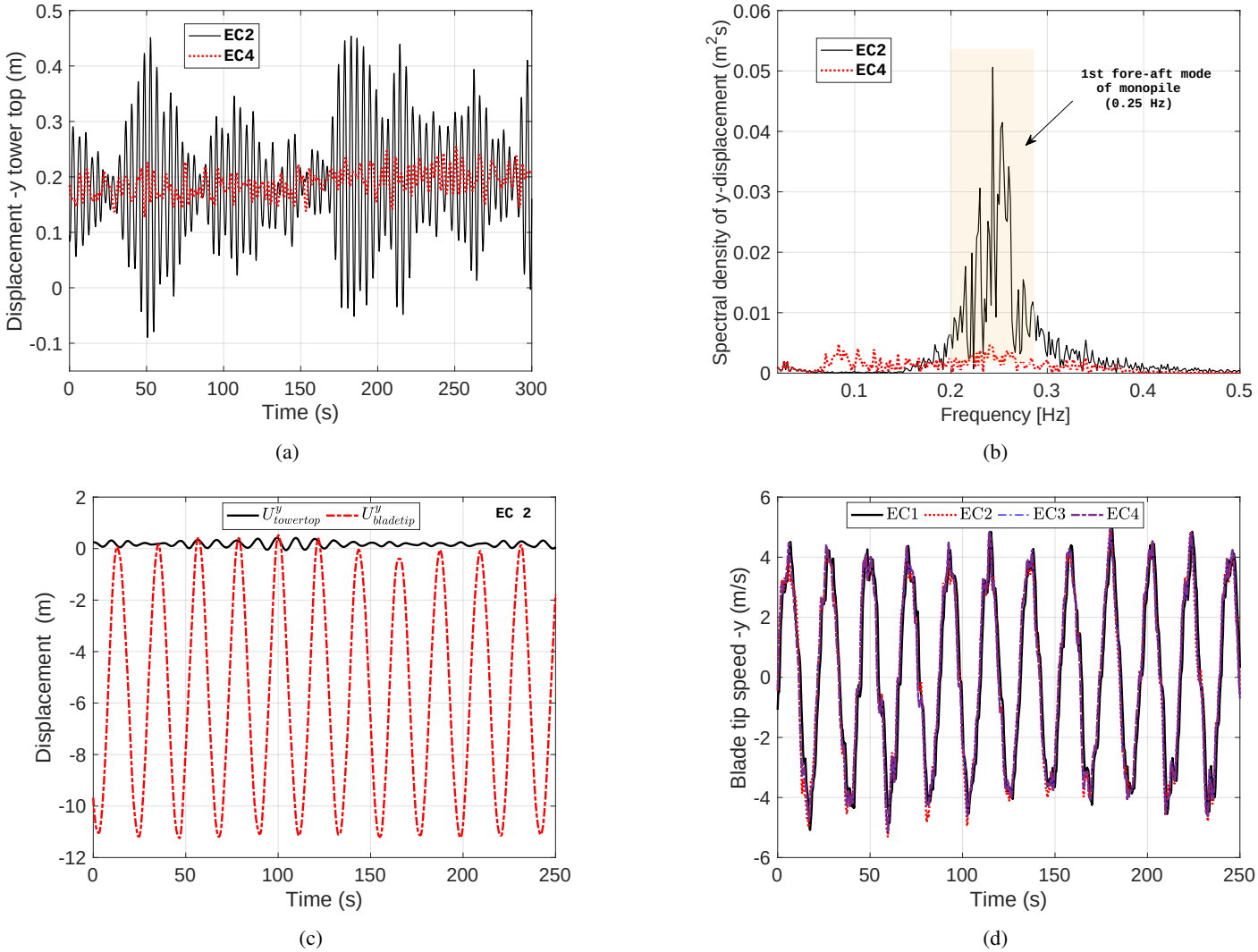

FIGURE 9: Comparison of (a) U^y_{hub} and its (b) Spectral density for EC2 and EC4; Comparison of (c) U^y_{hub} and U^y_{blade} (d) V^{blade}_y

erating at $U_w = 20m/s$ (i.e, above rated wind speed). Note that for all the cases of rainfall intensities and corresponding U_w, the droplet impact angle (α) varies, (see Figure 6(b)) and is considered in all the results presented hereafter. It can be seen from the figure that the highest impact velocity for all the cases is obtained at around $\theta = 270^o$, where V^{blade}_y and V^{blade}_z had their negative peak values (as discussed previously). A magnified view is also presented in Figure 8(b) showing the differences in the impact velocity for different rainfall intensities, which are found in the range of 5-10%. From the figure, there might be thoughts that there are not much differences in the impact velocities of the blade tip for different rainfall intensities, and that only the blade tip speed dominates erosion while operating at a given wind speed. However, it is to be noted that the erosive parameters, especially erosion damage rate ($\dot{D}_i$) is proportional to $\vec{V}_{imp}$ with a power of 6.7 (see eq. (5)). Therefore, even a modest increase in the impact velocity is expected to increase the $\dot{D}_i$ substantially. This can be seen from Figure 8(c), where erosion damage rate is compared for blade tip (considering material properties of PET coating listed in Table 1) at different rainfall intensities, different θ and $U_w = 20m/s$. The results clearly show that there is a substantial increase in the $\dot{D}_i$, which is more than 85% when exposed to very heavy rainfall compared to blades exposed to light rainfall. These results clearly demonstrate that for a given blade tip speed, different magnitude of rainfall intensity is expected to have varying rain erosion performance. Thus, these aspects need to be considered while developing control algorithm for reducing the tip speed of the blade. In this way, the incubation period ($1/\dot{D}_i$) of the blade can be extended. Figure 8(d) further presents the comparison between the peak im-

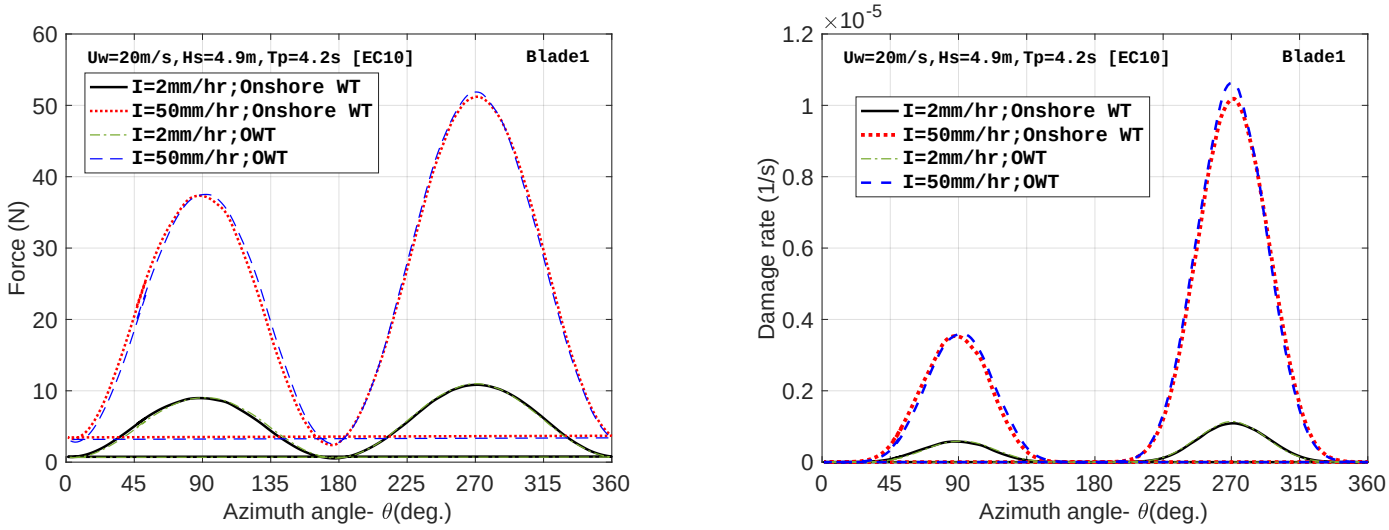

(a) (b)

FIGURE 10: Comparison of (a) F_{imp} (b) $\dot{D}_i$, between onshore and OWT for EC10 ($H_s = 4.9m, T_p = 4.2s, U_w = 20m/s$) and $I = 2mm/hr,\ 50mm/hr$

pact forces caused between the rotating blade tip ($r = 61.5m$) and rain droplet corresponding to different rainfall intensities ($I = 2mm/hr\ 10mm/hr\ 25mm/hr\ 50mm/hr$). Given that the peak force is proportional to $\vec{V}_{imp}$ with a power of 2 (see eq.(5)), a noticeable difference can be seen in the peak forces developed by heavy rainfall compared to light rainfall at different θ. Overall, $\dot{D}_i$ as well as other erosion parameters due to varying I are essential to be included for LEE analysis.

III. Effects of wave-induced monopile motions (H_s, T_p)

In this section, the effects of wave-induced loads on the LEE of WTBs in terms of $|\vec{V}_{imp}|$, and damage erosion rate ($\dot{D}_i$) will be discussed. Since collinear wind-wave conditions are considered in the study, only the motion of monopile in the fore-aft direction will affect the results for $|\vec{V}_{imp}|$ and are discussed hereafter. Figure 9(a) compares the motion of monopile in the fore-aft direction (y-global) for a load case corresponding to $H_s = 2.30m$, $T_p = 4.2s$ (EC2) and $H_s = 2m$, $T_p = 12s$ (EC4) together with a constant $U_w = 6m/s$, $TI = 0.06$ (below rated). It can be seen that the monopile has large responses in the fore-aft direction compared to $T_p = 12s$ and this is due to the fact that $T_p = 4.2s$ matches with the eigenfrequency of the turbine, thereby causing resonance. A spectral density curve for the monopile motion is compared for EC2 and EC4 in Figure 9(b), where high peak is seen at the the resonance frequency for load case EC2. Nevertheless the motion is still minor compared to the motion of the blade itself in the y-direction. This is due to the presence of aerodynamic damping from the rotating blades which reduces the amplification of responses at the resonance. For instance, Figure 9(c) compares the motion of monopile and blade in the global y-direction, and it is evident that the contribution of the monopile is minor. This implies that the wave-induced monopile motion is not expected to significantly change V_y^{blade}. This can be confirmed from Figure 9(d), where the V_y^{blade} is compared for EC1,EC2, EC3 and EC4, where EC1 corresponds to the case of onshore wind turbine. The contribution of wave-induced loads is negligible as the results for all the load cases completely overlap with each other except EC2, which exhibits a minor difference due to resonance effects discussed above.

Subsequently, the impact forces and damage erosion rates are compared (Figures 10(a)-(b)) between onshore and OWT for EC10. This case is the most critical for OWT due to large wave height ($H_s = 4.9m$) and $T_p = 4.2s$ which matches the resonance frequency. These results are presented for two different rainfall intensities ($I = 2mm/hr; 50mm/hr$), above rated wind speed ($U_w = 20m/s$) and $TI = 0.12$. The results show that the differences in the impact forces and damage erosion rate is minor for onshore and OWT for very heavy rainfall conditions, and is found negligible for light, moderate and heavy rainfall conditions. Overall, it can be implied from the results that the LEE erosion is not affected by wave-induced motions - therefore this parameter is not essential for LEE of WTBs. Note that the present paper only considers monopile-based fixed OWTs. These results will be compared in the future for floating OWTs.

IV. Effects of turbulence intensity (TI)

In this section, the effects of TI on the LEE are discussed. Figure 11(a) compares the velocity of the rotating blade in the global y-direction, for three $TI = 0.0,\ 0.12,\ 0.26$ and $U_w = 20m/s$. It is evident from the figure that considering just the

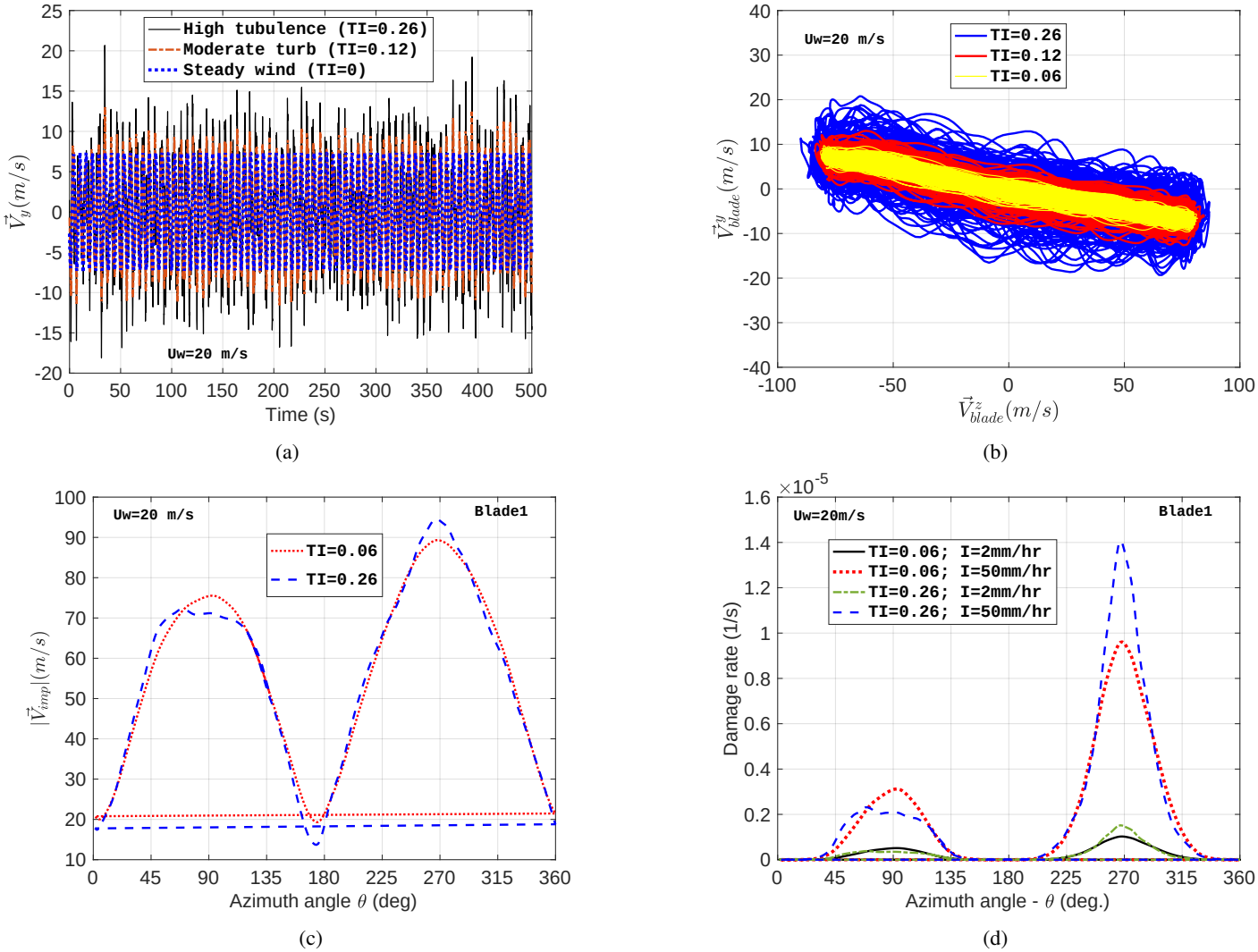

FIGURE 11: Comparison of (a) V_y^{blade} (b) blade tip speed in yz-plane (c) $|\vec{V}_{imp}|$ (d) $\dot{D}_i$ for $TI = 0.06,\ 0.12,\ 0.26$, and $U_w = 20m/s$

steady wind for the LEE analysis, underpredicts V_y^{blade}. Furthermore, peak values for V_y^{blade} increases from 7 m/s for $TI = 0.0$ to more than 20 m/s for $TI = 0.26$ - thereby implying the significance of TI for LEE modelling. Similar observations can be seen in Figure 11(b) where velocity of the lifted blade in the critical yz-plane are compared for $TI = 0.06,\ 0.12,\ 0.26$, and $U_w = 20m/s$. It can be seen from the figure that the V_y^{blade} increases with increasing TI, and there are minor influences on the V_z^{blade}. Further, Figure 11(c) compares the $|\vec{V}_{imp}|$ for two $TI = 0.06,\ 0.26$ and at θ. The difference in $|\vec{V}_{imp}|$ for both the cases is minor, however, there is a substantial influence on the erosion damage rate of LE. Figure 11(d) compares the $\dot{D}_i$ for ($TI = 0.06,\ 0.26$), and two rainfall intensities ($I = 2mm/hr,\ 50mm/hr$). The turbulence intensity is found to have significant influence on the erosion damage rate, and the effect is most critical for very heavy rainfall conditions ($I = 50mm/hr$) and high turbulent wind associated with gust conditions ($TI = 0.26$). Overall, TI is an important parameter to be included for LEE modelling. The results also show that current state of the art method, where steady power curve of wind turbine is included for the LEE analysis would underpredict the results.

CONCLUSION

The present paper performs aero-hydro-servo-elastic simulations on the rotating blade and investigate the influence of - (1) rainfall intensity (b) wave-induced loads, and (c) turbulence intensity, on the impact velocities and erosion damage rate of the leading edge. Different precipitation parameters are considered through an in-house code, and impact velocities are compared.

Analytical surface fatigue damage model are used to estimate erosion damage rate for a PET-based thermoplastic leading edge coating material. It is found that rainfall intensity and turbulence intensity influences the impact velocity minorly, however, has a substantial effect on the overall erosion damage rate. For instance, for the investigated load cases, an 8% increase in the impact velocity is observed when the turbulence intensity increases from 6% to 26%, which indicates an increase of erosion damage rate by more than 40%. Further, no substantial influence is found due to effects of wave-induced loads on the wind turbine.

LIMITATION AND FUTURE WORK

The investigations performed in this paper is limited to short-term analysis. Accurate evaluation of long-term LEE requires site-specific environmental data, information of the wind turbine operational condition, and a probabilistic framework. These aspects will be considered in the future work. Also, the springer model [11] used in this study for estimating erosion damage rate for the coating material needs to be validated, and further improved by considering factors such as- rest periods and viscoelastic properties of the elastomeric coatings. Further, given that the atmospheric stability conditions vary for onshore and offshore conditions, their effects on the erosion damage rate will be investigated in further studies. Also, all these investigations and results will be compared in the future for floating-based OWTs.

ACKNOWLEDGMENT

This work was made possible through the WINDCORE project having subsidy scheme TSE–18–04–01–Renewable energy project with project number TEHE1180113. The authors also appreciate anonymous reviewers for their kind comments which helped us to improve the quality of our work.

REFERENCES

[1] Verma, A. S., Vedvik, N. P., and Gao, Z., 2019. "A comprehensive numerical investigation of the impact behaviour of an offshore wind turbine blade due to impact loads during installation". *Ocean Engineering,* ***172***, pp. 127–145.

[2] Verma, A. S., Jiang, Z., Vedvik, N. P., Gao, Z., and Ren, Z., 2019. "Impact assessment of a wind turbine blade root during an offshore mating process". *Engineering Structures,* ***180***, pp. 205–222.

[3] Verma, A. S., Jiang, Z., Ren, Z., Gao, Z., and Vedvik, N. P., 2019. "Response-based assessment of operational limits for mating blades on monopile-type offshore wind turbines". *Energies,* ***12***(10), p. 1867.

[4] https://www.armouredge.com/. Picture taken.

[5] http://www.duraledge.dk. Photo by jakob ilsted bech, dtu wind energy.

[6] https://gcaptain.com/. Picture taken.

[7] Verma, A. S., Vedvik, N. P., Haselbach, P. U., Gao, Z., and Jiang, Z., 2019. "Comparison of numerical modelling techniques for impact investigation on a wind turbine blade". *Composite Structures,* ***209***, pp. 856–878.

[8] Verma, A. S., Zhao, Y., Gao, Z., and Vedvik, N. P., 2019. "Explicit structural response-based methodology for assessment of operational limits for single blade installation for offshore wind turbines". In Proceedings of the Fourth International Conference in Ocean Engineering (ICOE2018), Springer, pp. 737–750.

[9] Pineda, I., and Tardieu, P., Accessed: 2019-03-01. Wind in power 2018-annual combined onshore and offshore wind energy statistics.

[10] Pugh, K., Rasool, G., and Stack, M. M., 2019. "Raindrop erosion of composite materials: some views on the effect of bending stress on erosion mechanisms". *Journal of Bio-and Tribo-Corrosion,* ***5***(2), p. 45.

[11] Springer, G. S., 1976. "Erosion by liquid impact".

[12] Mishnaevsky Jr, L., 2019. "Repair of wind turbine blades: Review of methods and related computational mechanics problems". *Renewable energy*.

[13] Herring, R., Dyer, K., Martin, F., and Ward, C., 2019. "The increasing importance of leading edge erosion and a review of existing protection solutions". *Renewable and Sustainable Energy Reviews,* ***115***, p. 109382.

[14] Wiser, R., Jenni, K., Seel, J., Baker, E., Hand, M., Lantz, E., and Smith, A., 2016. "Forecasting wind energy costs and cost drivers: The views of the worlds leading experts".

[15] Slot, H., IJzerman, R., le Feber, M., Nord-Varhaug, K., and van der Heide, E., 2018. "Rain erosion resistance of injection moulded and compression moulded polybutylene terephthalate pbt". *Wear,* ***414***, pp. 234–242.

[16] Keegan, M. H., Nash, D., and Stack, M., 2014. "Wind turbine blade leading edge erosion: An investigation of rain droplet and hailstone impact induced damage mechanisms". PhD thesis, University of Strathclyde.

[17] Eisenberg, D., Laustsen, S., and Stege, J., 2018. "Wind turbine blade coating leading edge rain erosion model: Development and validation". *Wind Energy,* ***21***(10), pp. 942–951.

[18] Bech, J. I., Hasager, C. B., and Bak, C., 2018. "Extending the life of wind turbine blade leading edges by reducing the tip speed during extreme precipitation events". *Wind Energ. Sci. Discuss*.

[19] Chen, J., Wang, J., and Ni, A., 2019. "A review on rain erosion protection of wind turbine blades". *Journal of Coatings Technology and Research,* ***16***(1), pp. 15–24.

[20] Wang, Y., Deng, Y., Liu, Y., Qu, L., Wen, X., Lan, L., and Wang, J., 2019. "Influence of blade rotation on the lightning stroke characteristic of a wind turbine". *Wind Energy*.

[21] Amirzadeh, B., Louhghalam, A., Raessi, M., and Tootkaboni, M., 2017. "A computational framework for the anal-

ysis of rain-induced erosion in wind turbine blades, part i: Stochastic rain texture model and drop impact simulations". *Journal of Wind Engineering and Industrial Aerodynamics,* ***163***, pp. 33–43.

[22] Verma, A. S., Castro, S. G., Jiang, Z., and Teuwen, J. J., 2020. "Numerical investigation of rain droplet impact on offshore wind turbine blades under different rainfall conditions: A parametric study". *Composite Structures*, p. 112096.

[23] Keegan, M. H., Nash, D., and Stack, M., 2013. "On erosion issues associated with the leading edge of wind turbine blades". *Journal of Physics D: Applied Physics,* ***46***(38), p. 383001.

[24] Castorrini, A., Corsini, A., Rispoli, F., Venturini, P., Takizawa, K., and Tezduyar, T. E., 2016. "Computational analysis of wind-turbine blade rain erosion". *Computers & Fluids,* ***141***, pp. 175–183.

[25] De Lima, J., 1989. "The influence of the angle of incidence of the rainfall on the overland flow process". *IAHS Publication (United Kingdom)*.

[26] Best, A., 1950. "The size distribution of raindrops". *Quarterly Journal of the Royal Meteorological Society,* ***76***(327), pp. 16–36.

[27] Herring, R., Dyer, K., Howkins, P., and Ward, C., 2020. "Characterisation of the offshore precipitation environment to help combat leading edge erosion of wind turbine blades". *Wind Energy Science Discussions,* ***2020***, pp. 1–16.

[28] Larsen, T. J., and Hansen, A. M., 2007. "How 2 HAWC2, the user's manual".

[29] Jonkman, J., Butterfield, S., Musial, W., and Scott, G., 2009. "Definition of a 5-mw reference wind turbine for offshore system development". *National Renewable Energy Laboratory, Golden, CO, Technical Report No. NREL/TP-500-38060*.

[30] Zhang, R., Zhang, B., Lv, Q., Li, J., and Guo, P., 2019. "Effects of droplet shape on impact force of low-speed droplets colliding with solid surface". *Experiments in Fluids,* ***60***(4), p. 64.

[31] Zhang, B., Li, J., Guo, P., and Lv, Q., 2017. "Experimental studies on the effect of reynolds and weber numbers on the impact forces of low-speed droplets colliding with a solid surface". *Experiments in Fluids,* ***58***(9), p. 125.

[32] Verma, A. S., 2019. "Modelling, Analysis and Response-Based Operability Assessment of Offshore Wind Turbine Blade Installation with Emphasis on Impact Damages". PhD Thesis, Norwegian University of Science and Technology (NTNU), Trondheim.

[33] Jonkman, J., and Musial, W., 2010. Offshore code comparison collaboration (oc3) for iea wind task 23 offshore wind technology and deployment. Tech. rep., National Renewable Energy Lab.(NREL), Golden, CO (United States).

[34] Shirzadeh, R., Devriendt, C., Bidakhvidi, M. A., and Guillaume, P., 2013. "Experimental and computational damping estimation of an offshore wind turbine on a monopile foundation". *Journal of Wind Engineering and Industrial Aerodynamics,* ***120***, pp. 96–106.

[35] Morison, J., Johnson, J., Schaaf, S., et al., 1950. "The force exerted by surface waves on piles". *Journal of Petroleum Technology,* ***2***(05), pp. 149–154.

[36] Verma, A. S., Gao, Z., Jiang, Z., Ren, Z., and Vedvik, N. P., 2019. "Structural safety assessment of marine operations from a long-term perspective: A case study of offshore wind turbine blade installation". In ASME 2019 38th International Conference on Ocean, Offshore and Arctic Engineering, American Society of Mechanical Engineers Digital Collection.

[37] Madsen, H. A., Riziotis, V., Zahle, F., Hansen, M. O. L., Snel, H., Grasso, F., Larsen, T. J., Politis, E., and Rasmussen, F., 2012. "Blade element momentum modeling of inflow with shear in comparison with advanced model results". *Wind Energy,* ***15***(1), pp. 63–81.

[38] Pirrung, G. R., Madsen, H. A., Kim, T., and Heinz, J., 2016. "A coupled near and far wake model for wind turbine aerodynamics". *Wind Energy,* ***19***(11), pp. 2053–2069.